Available online at www.sciencedirect.com
ScienceDirect
Journal of Solid State Chemistry 180 (2007) 3388–3392
JOURNAL OF SOLID STATE CHEMISTRY
www.elsevier.com/locate/jssc

$Ba_2In_2O_4(OH)_2$: Proton sites, disorder and vibrational properties

Jean-Raphaël Martinez[a], Chris E. Mohn[a], Svein Stølen[a,*], Neil L. Allan[b]

[a]*Department of Chemistry and Centre for Nanotechnology and Materials Science, University of Oslo, Postbox 1033, Blindern, N0315 Oslo, Norway*
[b]*School of Chemistry, University of Bristol, Cantock's Close, Bristol BS8 1TS, UK*

Received 7 June 2007; received in revised form 31 August 2007; accepted 29 September 2007
Available online 11 October 2007

Abstract

The structure of $Ba_2In_2O_4(OH)_2$ is analysed by the explicit full optimization of a large number of possible proton arrangements using periodic density functional theory. It is shown that the experimental assignments in which protons appear to be located at high symmetry positions with unphysical bond lengths do not correspond to minima on the potential energy hypersurface. The apparent sites are averages of a number of possible proton locations involving a set of possible local structural environments in which the internuclear separations are more realistic. Such problems with structural refinements are common where profile refinement programs place the atoms at the average position due to dynamic and/or static disorder. Thus while the calculations support a previous neutron diffraction analysis of the structure in that the *average* structure contains two different proton sites, they also reveal substantial information about the local environments of the protons. In all optimizations, the protons moved from the average positions suggested in the neutron diffraction study with calculated O–H and OH···O distances consistent with those observed in other oxides. The energies of different proton distributions vary significantly so the protons are not randomly distributed. We also present an analysis of the vibrational properties of the O–H bonds. Since the strength of the hydrogen bonds is closely related to the local structural environments of the protons, a range of vibrational frequencies is obtained providing a prediction of the vibrational spectra. In O–H···O linkages, O–H stretching modes soften with increasing H···O hydrogen bond strength, while the in-plane and out-of-plane bending or libration modes stiffen. Together, our results show how modern theoretical methods can provide a clearer understanding of the structure and dynamics of a complex inorganic material.

Keywords: $Ba_2In_2O_4(OH)_2$; Protons; Protons in oxides; Vibrational properties; Disorder; DFT; Local structure; Crystal structure

1. Introduction

$Ba_2In_2O_5 \cdot H_2O$ was first characterized structurally by *in-situ* high-temperature powder X-ray diffraction [1]. This study was unable to determine the proton sites accurately and the structure was recently reinvestigated by a combination of ^1H and ^2D NMR, electron, X-ray and neutron diffraction [2], suggesting that the phase is best described as an oxyhydroxide, $Ba_2In_2O_4(OH)_2$. Here we present a density functional theory study of $Ba_2In_2O_4(OH)_2$, concentrating on proton location, disorder and the vibrational properties of the O–H bonds, by investigating many possible proton arrangements. A primary aim is to characterize the structure and, in particular, to investigate the different sites over which the protons are distributed in order to establish whether the protons are randomly distributed or exhibit a preference for particular arrangements. A second objective is to study the hydrogen bonding with emphasis on vibrational properties. Enhanced hydrogen bonding reduces the stretching frequency of the O–H bond since the hydrogen bond acceptor shifts the proton away from the donor atom and lowers the O–H bond strength [3]. Since the strength of the hydrogen bonds are closely related to the local structural environments of the protons in the compound, a range of frequencies is expected [3,4].

The structure of $Ba_2In_2O_4(OH)_2$ can be understood using that of perovskite as a starting point. All InO_6 octahedra share corners and form a three-dimensional network. The neutron diffraction study suggests that the protons occupy two crystallographically distinct sites

*Corresponding author. Fax: +47 2285 5441.
E-mail address: svein.stolen@kjemi.uio.no (S. Stølen).

0022-4596/$ - see front matter © 2007 Elsevier Inc. All rights reserved.
doi:10.1016/j.jssc.2007.09.034

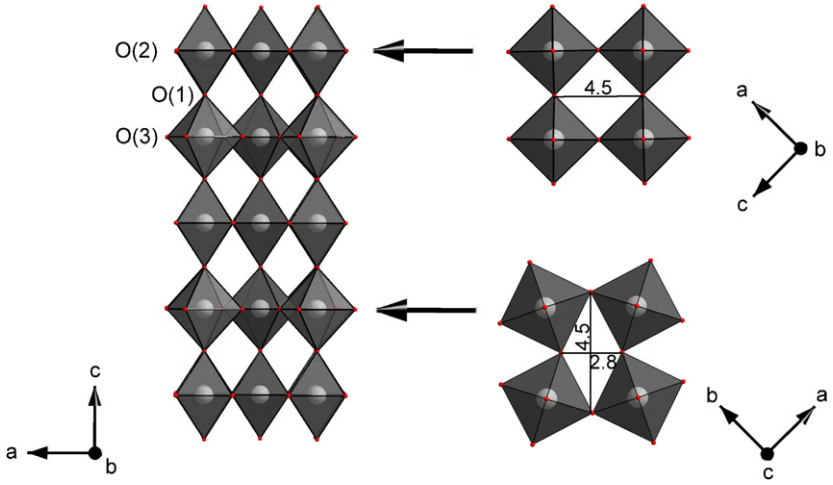

Fig. 1. Polyhedron representation of the $Ba_2In_2O_4(OH)_2$ structure showing the arrangement of the InO_6-octahedra.

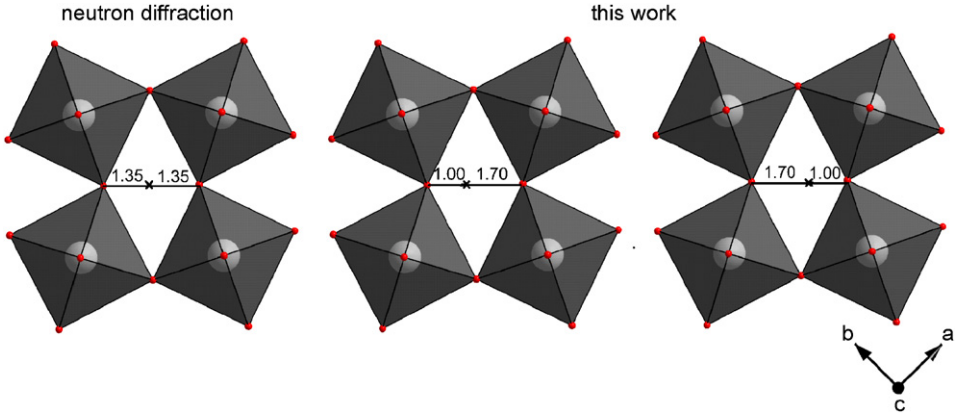

Fig. 2. Proton sites in the *B*-layer: (a) average 2*c* position suggested by neutron diffraction [2] and (b) presently obtained 4*h* positions.

giving rise to a tetragonal structure with $a=b=5.915$ Å, $c=8.999$ Å [2]. The unit cell contains two formula units and two different layers of octahedra arranged in a *ABABAB*… stacking sequence along the *c*-axis (see Fig. 1). There are three distinct oxygen sites, also shown in Fig. 1. O(1) atoms are apical oxygens. The oxygen atoms in the equatorial planes of the *A*- and *B*-layers occupy O(2) and O(3) sites, respectively. The *A*-layer contains octahedra in which the O(2)–O(2) distance is 4.5 Å and the O(2)–O(2)–O(2) angles are close to 90°, whereas the octahedra in the *B*-layers are tilted such that the O(3)–O(3) distances are 2.8 and 5.8 Å and O(3)–O(3)–O(3) angles are 58° and 132° (see Fig. 1).

The neutron diffraction study [2] concluded that the protons are found at 2*c* and 16*l* sites. The 2*c* site is located in the *B*-layer at the midpoint between neighbouring equatorial O(3) atoms giving (on average) two O(3)–H bonds with bond lengths of 1.35 Å (Fig. 2). It was, however, stressed that this 2*c* position probably represents the average position of a proton jumping between two 4*h* sites closer to each O(3) positions [2]. The 16*l* positions are all in the planes formed by the apical oxygen atoms perpendicular to the *c*-axis. In the unit cell there are two such planes each containing eight such

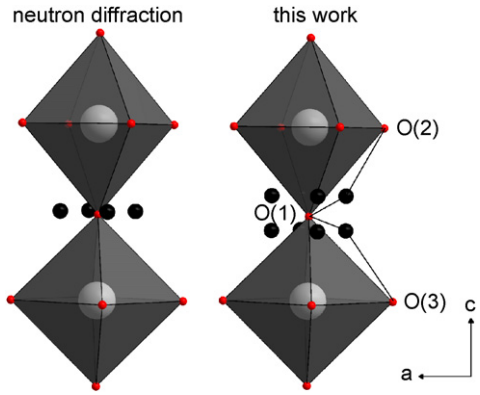

Fig. 3. Proton sites close to the apical O(1) atoms: (a) 16*l* positions suggested by neutron diffraction [2] and (b) presently obtained "32*y*" positions.

positions (Fig. 3). The shortest O(1)–H distance for a proton at a 16*l* position is 0.99 Å, giving O(1)H⋯O(2)/O(3) distances close to 2.49 Å. The neutron diffraction study [2] suggests the average 2*c* site is fully occupied and that the 16*l* site has a fractional occupancy of 1/8.

2. Computational details

All structural optimizations and calculations of vibrational frequencies are carried out using density functional theory within the general gradient approximation (using the Perdew–Wang-91 functional [5]) as implemented in the Vienna *ab-initio* simulation programme (VASP) [6,7]. We use a 3*3*3 *k*-point mesh and a high constant energy cut-off (649 eV) in the present work. Test calculations indicate that the vibrational frequencies increases by less than $20\,cm^{-1}$ when increasing the *k*-mesh from 3*3*3 to 4*4*4.

The structural optimizations were performed without any constraint on the atomic positions, the cell shape or the cell volume and were accompanied by significant structural relaxations. Due to changes in the volume and cell-shape during optimizations of the individual arrangements we carried out additional re-optimizations starting from the relaxed configurations to ensure that the forces are sufficiently converged for the calculation of the vibrational frequencies.

The finite displacement method [8] is used for the construction of the dynamical matrix of each of the individual configurations at the Γ-point and involves displacing each atom 0.02 Å along the three Cartesian directions in both positive and negative directions within the *primitive* cell of the optimized arrangement. The diagonalization of the dynamical matrix provides polarization vectors and frequencies of the 3*N* normal modes of (*N* is the number of atoms in the primitive cell of a particular configuration). The splitting of optical modes to transverse (TO) and longitudinal (LO) components is neglected.

In order to study different possible distributions of the H-atoms in the crystal structure we used the neutron diffraction study [2] as a starting point for the structural optimizations. For a 24-ion simulation cell we have 120 different possible arrangements of the four protons, assuming the experimental result that the 2*c* position is fully occupied. Since many of these arrangements are symmetrically equivalent we can reduce the number of optimizations—and hence the computational cost—by identifying a complete set of symmetrically *non-equivalent* initial arrangements [9,10]. Of the 120 initial arrangements, there are only 14 symmetrically non-equivalent initial arrangements (excluding sites that are too close to be simultaneously occupied). In order to confirm that the 2*c* site is fully occupied we also carry out six additional calculations starting from configurations where one or both 2*c* positions are vacant (implying a larger occupancy of the 16*l* position).

3. Results and discussion

3.1. Structure

We carried out full structural optimizations of the 20 symmetrically non-equivalent configurations (six of these are configurations where the 2*c* is partially occupied and 14 in which the 2*c* is fully occupied). Where optimization started from configurations in which the 2*c* site were not fully occupied, the final energies after optimization were all high, and the distinction between the *A*- and *B*-layers of the structure disappears. This supports the model suggested by the diffraction data [2] of an average structure with a fully occupied 2*c* site and a partially occupied 16*l* site. However, in all the optimizations, the protons moved from the average positions suggested by the neutron diffraction analysis [2] and thus the calculated O–H and OH···O distances differ significantly from the average neutron diffraction values.

In the optimized structures the protons occupy the 4*h* site suggested by Jayaraman et al. [2] with one position lying on each side of the 2*c* site between the neighbouring equatorial oxygen atoms of different octahedra in the *B*-plane, as shown in Fig. 2. The free parameter *x* of the 4*h* site is about 0.04. The result is a O(3)–H distance close to 1.00 Å and a O(3)H···O(3) distance of $\approx$1.70 Å. The average of these (1.35 Å) agrees well with the average value reported in the neutron diffraction study. To see if the barrier between these two minima is thermally accessible we have also estimated the height of this barrier associated with proton transfer between the two O(3) atoms, assuming the 2*c* position is close to the transition state. The proton was first placed at the 2*c* position of the optimized structure (see Fig. 2a), giving a barrier $\approx$0.4 eV. Subsequent relaxation of the structure, keeping the O–H distance fixed reduces the barrier height to $\approx$0.1 eV. Such a barrier height indicates a dynamic equilibrium between the two positions at least at 1000 K. It is worth noting that neighbouring 4*h* positions are so close together that they cannot both be occupied simultaneously.

The hydrogen atoms which the neutron study [2] suggests occupy the 16*l* site also relax considerably from their initial positions. While the 16*l* site corresponds to four equivalent average positions around a specific O(1) ion, the present calculations suggest there are eight possible "equivalent" positions for the protons as illustrated in Fig. 3. We refer to these new positions close to the 16*l* site as "32*y*". They are defined from the 4*e* positions taken by the O(1) atoms by the eight displacements given by ($\pm$0.4, $\pm$0.4, $\pm$0.4 Å).

The shortest O–H distance involving a "32*y*" proton is close to 1.00 Å. The protons involved form hydrogen bonds with OH···O distances close to 1.90 Å and are thus weaker than those involving the 4*h* positions considered above. Studies [11] of protons in oxides in general give O–H distances close to 1.0 Å, while the O–H···O hydrogen bonds typically are around 1.8 Å and the O–H···O angles close to 125°. The discrepancy between the average experimental O(1)–H···O(1) distance (2.5 Å) and the calculated value of 1.9 Å results from the significant relaxation of the protons from the 16*l* site. Neither the O(1)–H bond nor the hydrogen bond are perpendicular to the *c*-direction. As a result the hydrogen bond involves not

O(1) but to O(2) or O(3) as indicated by the dashed lines in Fig. 3.

For most configurations, the O–H bond involves O(1)-ions. Configurations where the O–H bonds involves the O(2)-site are also minima on the potential energy surface but these are high in energy and thus thermally inaccessible. The lowest energy configuration of these with one of the two "32*y*" protons bonded to a O(2) is 0.8 eV per unit cell above the ground state configuration. Thus protons bonded to oxygens occupying O(1) positions are not easily transferred to positions in which the hydrogen is then bonded to an O(2) oxygen.

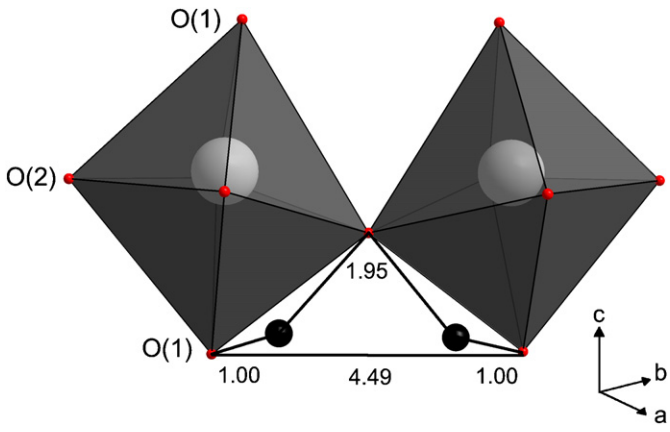

Fig. 4. Arrangement of the two "32*y*" protons in the lowest energy configuration.

Different representative distributions of the two protons over the "32*y*" site are shown in Figs. 4 and 5. In the lowest energy configuration (Fig. 4) the two "32*y*" protons are clustered together such that they form short bonds to neighbouring O(1) atoms. Furthermore, they form hydrogen bonds to the same O(2) atom. This common O(2)-atom is strongly displaced in the *c*-direction compared to its average position obtained by neutron diffraction. Examples of higher energy configurations are given in Figs. 5a–e in order of increasing energy. While configurations represented in Fig. 5a have energies in the range 0.02–0.07 eV above the ground state, Fig. 5b–d configurations have energies in the range 0.2–0.3 eV. Fig. 5e configurations are significantly higher in energy, around 0.8 eV above the ground state.

3.2. Vibrational frequencies

Fig. 6 shows the characteristic O–H vibrational modes at the Γ point as a function of the OH···O hydrogen bond length. In general the modes are not pure stretches or bends, and some involve more than one proton moving significantly at the same time, but nevertheless it is generally possible to assign individual modes as predominantly stretching, in-plane or out-plane bending. Since the degree of hydrogen bonding is associated with the local structural environment of the protons a range of frequencies is observed. In general terms, due to the hydrogen bonds, O–H stretching modes soften, while the in-plane

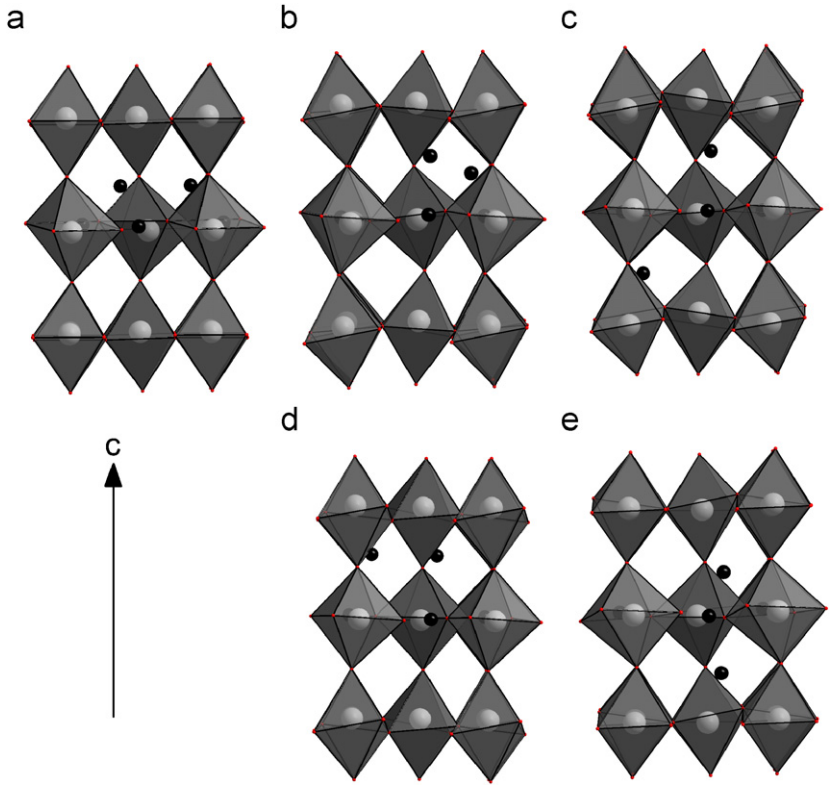

Fig. 5. Higher energy configurations in order of increasing energy. The *B*-layer is "fully" occupied by 2 protons, the remaining 2 protons are bond to O(1) atoms. One of the two protons at the 4*h* site is hidden behind an octahedra and thus not seen.

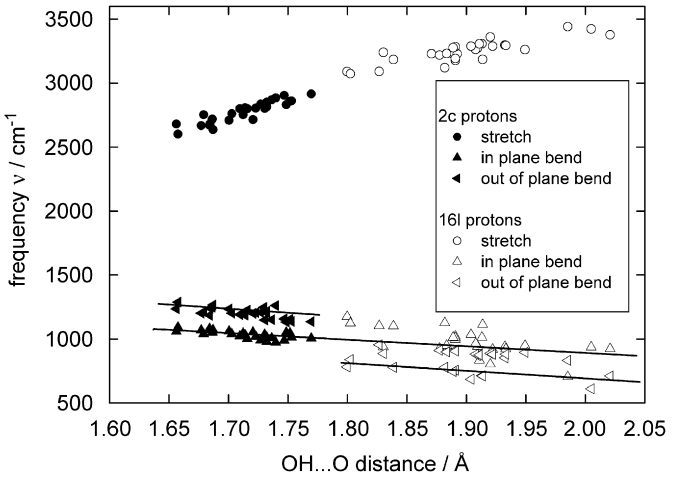

Fig. 6. The characteristic O–H vibrational modes as a function of the OH···O hydrogen bond length.

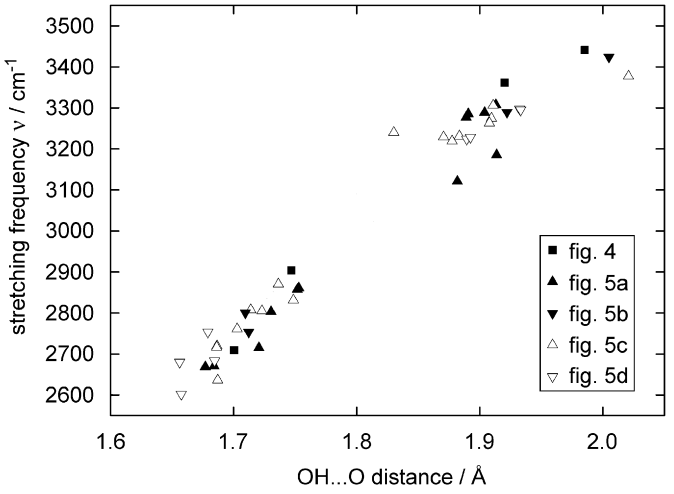

Fig. 7. The characteristic O–H stretching modes as a function of the OH···O hydrogen bond length. Values shown are for the configurations represented by Figs. 4 and 5a–d.

and out-of-plane bending or libration modes stiffen [3], the so-called 'tension' effect [12]. The lowering of the stretching frequency of the O–H bond with increasing hydrogen bonding is due to the attractive force of the hydrogen bond acceptor which shifts the proton further from the donor atom, increases the O–H bond length and so weakens the effective stretching force constant. The stiffening of the bending modes arises similarly. As the hydrogen bond strength increases the frequencies of the bends increases.

Fig. 7 show more details for the stretching modes in that the frequencies of the configurations in Figs. 4 and 5a–d are distinguished. The high-energy configurations represented by Fig. 5e are not included in the graph since they are not thermally accessible. We predict that the IR/Raman spectra of the compound will be dominated by two peaks; one roughly centred at 2800 cm^{-1} and one at around 3300 cm^{-1}. The former is due to protons in the 4*h* site, the latter at the "32*y*" site. This may explain the appearance of IR bands in hydrated $BaIn_xZr_{1-x}O_{3-x/2}$ with increasing indium content [13].

4. Final remarks

In this paper, we have studied the structure and dynamics of $Ba_2In_2O_4(OH)_2$ by the explicit full optimization of a large number of possible proton arrangements using periodic density functional theory. The results have highlighted the importance of the local proton environments and their symmetries—indeed the sites reported experimentally for the protons do not even correspond to minima on the potential energy hypersurface. Whilst the *average* structure observed experimentally contains two different proton sites, and is consistent with our calculations, this average reveals nothing about the local environments of the protons. There are strong energetic preferences for particular local structures and the protons are not randomly distributed. These structural correlations may at low temperatures extend beyond the boundary of the simulation cell used in this study, which would be consistent with the existence of larger superstructures observed by selected area electron diffraction [2]. Overall our results show how modern theoretical methods can provide a clearer understanding of the structure and dynamics of a complex inorganic material.

Acknowledgments

This work was funded by the Research Council of Norway. The Research Council of Norway (Programme for Supercomputing) has also supported the work through a grant of computing time.

References

[1] W. Fischer, G. Reck, T. Schober, Solid State Ion. 116 (1999) 211.
[2] V. Jayaraman, A. Magrez, M. Caldes, O. Joubert, F. Taulelle, J. Rodriguez-Carvajal, Y. Piffard, L. Brohan, Solid State Ion. 170 (2004) 25.
[3] W.O. George, Rh. Lewis, Hydrogen bonding in handbook of vibrational spectroscopy, in: P.R. Griffiths, J.M. Chalmers (Eds.), Sample Characterization and Spectral Data Processing, vol. III, Wiley, New York, 2002, pp. 1919–1934.
[4] E. Libowitzky, Monatsh. Chem. 130 (1999) 1047.
[5] J.P. Perdew, Y. Wang, Phys. Rev. B 45 (1992) 13244.
[6] G. Kresse, J. Hafner, Phys. Rev. B 47 (1993) 558.
[7] G. Kresse, J. Furthmüller, Phys. Rev. B 54 (1999) 11169.
[8] D. Alfe, G.A. de Wijs, G. Kresse, M.J. Gillan, Int. J. Quant. Chem. 77 (2000) 871.
[9] E. Bakken, N.L. Allan, T.H.K. Barron, C.E. Mohn, I.T. Todorov, S. Stølen, Phys. Chem. Chem. Phys. 5 (2003) 2237.
[10] I.T. Todorov, N.L. Allan, M.Y. Lavrentiev, C.L. Freeman, C.E. Mohn, J.A. Purton, J. Phys.: Condens. Matter 16 (2004) S2751.
[11] W. Münch, K.-D. Kreuer, G. Seifert, J. Maier, Solid State Ion. 125 (1999) 39.
[12] G.D. Barrera, J.A.O. Bruno, T.H.K. Barron, N.L. Allan, J. Phys.: Condens. Matter 17 (2005) R217.
[13] M. Karlsson, M.E. Björketun, P.G. Sundell, A. Matic, G. Wahnström, D. Engberg, L. Börjesson, I. Ahmed, S. Erikson, P. Berastegui, Phys. Rev. B 72 (2005) 094303.